Mode spectrum characteristics and onset of the low-shear MHD stability regime

A. M. Wright and N. M. Ferraro
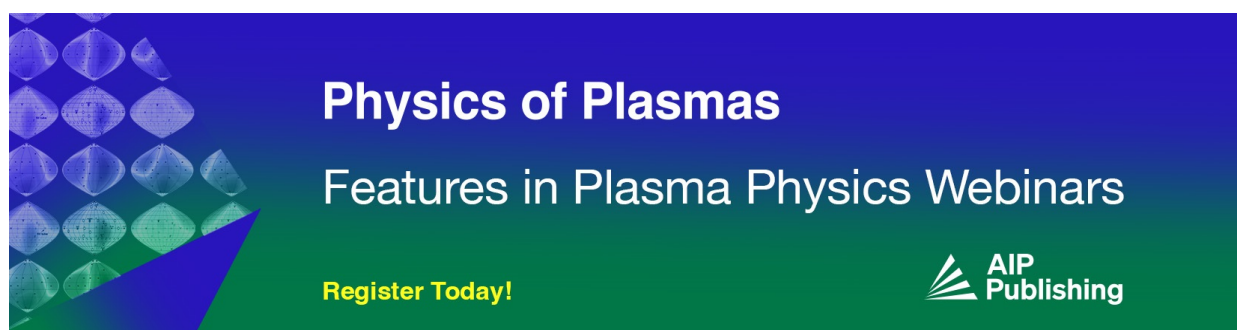
View Online   Export Citation   CrossMark

ARTICLES YOU MAY BE INTERESTED IN

Physics of Plasmas

Features in Plasma Physics Webinars

Register Today!

AIP Publishing

Mode spectrum characteristics and onset of the low-shear MHD stability regime

View Online   Export Citation   CrossMark

A. M. Wright[a] (iD) and N. M. Ferraro (iD)

AFFILIATIONS

Princeton Plasma Physics Laboratory, Princeton, New Jersey 08543, USA

[a]Author to whom correspondence should be addressed: awright@pppl.gov

ABSTRACT

Equilibria with extended regions of weak magnetic shear, including some tokamak scenarios and stellarators, can be susceptible to pressure-driven internal MHD instabilities even though there is no mode rational surface in the plasma. Nonresonant modes, in particular, can have properties that are unattractive for confinement, including displacing substantial volumes of the plasma and leading to more efficient pressure gradient flattening in the nonlinear regime. The onset and linear properties of the low shear stability regime are examined using the initial-value, extended-MHD code M3D-C[1]. For monotonic q-profiles, we demonstrate a clear correlation between the convergents associated with the continued fraction representation of q_0 and the spectrum of unstable modes. Nonresonant modes are observed to be destabilized preferentially to any other resonant instability with the same toroidal mode number when $n > 1$. Using the observed connection between the spectrum associated with q_0 and the overall equilibrium stability properties, we suggest a technique for reducing the uncertainty on both q_0 and magnetic shear in the core region, obtained either via measurement or through the analysis and reconstruction of experimental results.

Published under an exclusive license by AIP Publishing. https://doi.org/10.1063/5.0053870

I. INTRODUCTION

When magnetic shear is reduced over a significant volume in magnetically confined fusion plasmas, pressure-driven internal magnetohydrodynamic (MHD) modes that would otherwise be stabilized by magnetic shear can become unstable. An important subset of these is what we refer to as "nonresonant" modes, that is, internal modes for which there is no resonant surface in the plasma (i.e., $q \neq m/n$, where m and n are the poloidal and toroidal mode numbers, respectively). Nonresonant pressure-driven modes have global mode structures,[1,2] generating substantial plasma displacements, which may lead to efficient flattening of pressure gradients in the nonlinear regime. Under such circumstances, nonresonant modes can become an important determinant of stability boundaries and, consequently, affect the operational limits of fusion devices.

Equilibria with very flat central q-profiles and q_0 above one are characteristic of the "hybrid" class of advanced scenarios being explored en route to steady state operation in ITER.[3–8] Low shear profiles also play an important role in some proposed models of the sawtooth phenomenon,[9–11] particularly where an ideal ($m = 1, n = 1$) quasi-interchange mode is invoked as the crash progenitor. In some models, q_0 is close to but above unity.[10,11] For example, a recent model developed by Jardin et al.[11] proposes that, under certain conditions,

the crash is due to destabilization of and nonlinear interactions between nonresonant (n,n) interchange modes where $n > 1$. Of course, sawtooth models have been and continue to be the subject of much debate and on-going study (see, for example, Refs. 11 and 12 and references therein).

Modern day stellarators often have relatively flat rotational transform profiles, resulting in equilibria with low global magnetic shear.[13] Indeed, the island divertor concept of Wendelstein 7-X relies critically on low magnetic shear to achieve adequate separation between the confinement region and wall.[14] Since the plasma current in optimized stellarators is significantly reduced compared to tokamaks, pressure-driven instabilities take on renewed importance with respect to device performance.

Select properties of nonresonant pressure-driven modes have been studied previously in both tokamak and stellarator contexts,[1,15–17] including as ideal interchange and quasi-interchange modes. Infernal modes, a class of toroidal, pressure-driven instability that can appear in equilibria which satisfy the Mercier criterion and are ballooning-stable, were shown to reduce to interchange-like modes in the cylindrical limit.[18]

A perturbation analysis of the standard Energy Principle for the ($m = 1, n = 1$) mode in the cylindrical limit illustrated how

nonresonant modes can arise due to a global breakdown of the standard parameter ordering (which goes as ε^2, where ε is the inverse aspect ratio)[19] in low-shear equilibria.[16] This analysis was subsequently extended to higher order and for arbitrary poloidal and toroidal mode numbers.[20] In effect, the so-called nonresonance parameter,[20] $\delta q \equiv |q - m/n| \neq 0$, becomes another small parameter that can qualitatively modify the ordering which determines linear stability in the low-shear region.

A challenge common to both nonresonant and infernal modes[21] is to predict the toroidal and poloidal mode numbers most likely to be unstable. Even though $q \neq m/n$ in the former, it is intuitive to expect that an (m,n) mode might nonetheless be unstable if m/n is close enough to an extremal value of q in tokamaks or, equivalently, n/m to ι in stellarators. Excepting high-n ballooning modes, for internal modes it is expected that modes associated with low-order rational surfaces are likely to be key determinants of plasma stability.[21] However, in low shear equilibria there can exist conditions where moderate- to higher-n modes are similarly important.[18,20,21] Thus, it is essential to understand when nonresonant modes associated with low-order rationals, such as the $(m = 1, n = 1)$ or $(m = 4, n = 3)$ modes considered in previous studies,[10,11,16,18] are dominant over all other nonresonant modes with higher poloidal and toroidal mode numbers.

In this work, we examine the onset of the low shear stability regime and characteristics of the unstable mode spectrum using a recently introduced continued fraction approach[20] for low shear tokamak-like equilibria. The equilibrium profiles used throughout this study are described in Sec. II. In Sec. III, we discuss resonances and MHD stability from the perspective of the continued fraction representation of real numbers. We focus on convergents, which provide the best rational approximation of a given real number compared to all other fractions with smaller denominators. We describe how the mode spectrum associated with a partial sequence of convergents can be constructed from the continued fraction representation of q_0. This turns out to dominate the equilibrium stability characteristics in the low shear regime. In Sec. IV, we use the initial-value, extended-MHD code M3D-C^1 (described in Ref. 22) to study the linear properties and onset of nonresonant modes as a function of decreasing shear. In Sec. V, we demonstrate the preferential destabilization of nonresonant modes (and higher-order harmonics thereof) over any other resonant instability with the same toroidal mode number for $n > 1$ when magnetic shear is weak. In Sec. VI, we examine the effect of other nonresonant modes on the low-shear MHD stability regime. We posit that knowledge of the characteristic mode spectrum (derived from the continued fraction representation) can be potentially applied to systematically reduce the uncertainty on q_0 obtained, for example, via measurement or equilibrium reconstruction and address additional developments that are required to enable this approach. Finally, conclusions and implications are presented in Sec. VII.

II. EQUILIBRIUM PROFILES

In addition to generating substantial plasma displacements which may lead to greater pressure gradient flattening due to magnetic field line chaos generated via nonlinear interactions, nonresonant modes can also destabilize resonant modes through poloidal and toroidal mode coupling. Indeed, mode coupling that leads to the formation of additional magnetic islands and the subsequent generation of

magnetic field line chaos via island overlap has been proposed as a pathway to disruptions[23] and as part of a sawtooth crash mechanism.[11]

Being able to disentangle the "progenitor" modes from those which are secondarily destabilized by coupling effects can provide new insights on global MHD stability properties and enable efficient design of equilibria with desirable MHD stability properties. For this work we are, therefore, interested in the properties intrinsically associated with the resonant or nonresonant nature of the modes. As such, we seek to eliminate all poloidal and toroidal mode coupling as a potential source of instability drive.[2] Consequently, we consider a periodic cylinder, which models tokamak equilibria in the large aspect ratio limit. Since toroidal effects are reduced in the low-shear equilibria of interest, this is a reasonable model for the present purpose.[10]

Throughout this work, the q-profiles are given by

$$q = q_0 \left[1 + x^{2\lambda} \left(\left(\frac{q_a}{q_0} \right)^{\lambda} - 1 \right) \right]^{1/\lambda}, \tag{1}$$

where $x \equiv r/a$ is a normalized radial coordinate, a is the minor radius, q_0 and q_a denote the value of the safety factor at the magnetic axis and plasma edge, respectively, and λ is some constant. We fix $q_a = 3.38197$, $a = 1\,\mathrm{m}$, and set $R_0 = 3\,\mathrm{m}$ as the major radius, which corresponds to an aspect ratio of 3. The pressure profiles are given by

$$p = p_0 \left(1 - x^{\bar{\lambda}} \right)^{\bar{\lambda}}, \tag{2}$$

where p_0 is the pressure on the magnetic axis and $\bar{\lambda} = 2.5$. We prescribe q_0, q_a, and λ, and solve for p_0 such that the equilibrium satisfies a specified value of the average plasma β, which is given by

$$\beta = \frac{2\mu_0 \langle p \rangle}{\langle B^2 \rangle}, \tag{3}$$

where $\langle \cdot \rangle$ denotes a volume average and μ_0 is the vacuum permeability. This is the same approach taken by Manickam et al.,[21] for example, and chosen to readily enable comparison to existing results.

The parameter λ relates directly to the magnetic shear, allowing it to be continuously varied with a single parameter. In this study, we choose a sequence of values for λ such that the edge of the low shear region is approximately equally spaced in radius. The equilibrium q-profiles and toroidal current density profiles, J_z, are given in Fig. 1. We consider $1 \leq \lambda \leq 8$ with $\beta = 3\%$. Note that $\lambda = 1$ corresponds to a quadratic q-profile and serves as a convenient reference case.

III. IDENTIFYING THE MODE SPECTRUM ASSOCIATED WITH q_0

Building on ideas recently introduced by Wright et al.,[20] we demonstrate how the continued fraction representation of real numbers can be used to construct a mode spectrum associated with any q (or ι) that is unique, with two exceptions. Depending on whether q is interior to or coincides with the end point of the subset of $\mathbb{R}$ spanned by all qs in the plasma, the spectrum can include both resonant and nonresonant modes. For min q or max q, half the spectrum will consist of nonresonant modes. We will see in Secs. IV and V that the mode spectrum associated with q_0 is well correlated with the observed unstable modes when magnetic shear is weak. With these considerations in
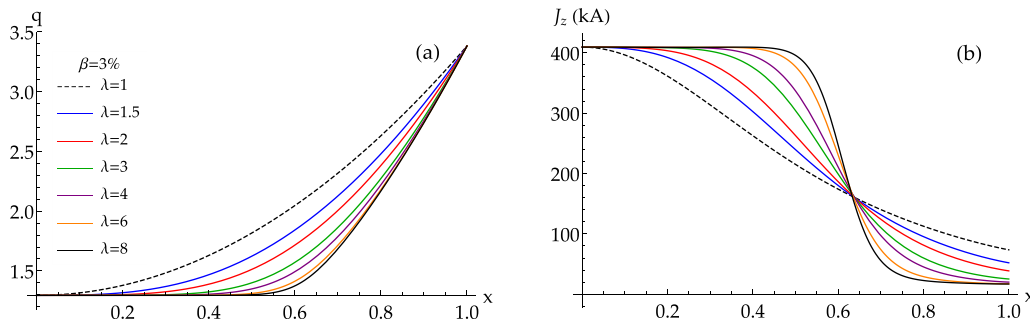
FIG. 1. (a) Equilibrium q-profiles and (b) toroidal current density profiles for $\beta = 3\%$ and $1 \leq \lambda \leq 8$ where λ controls the magnetic shear. The reference case, $\lambda = 1$ (dashed line), corresponds to a quadratic q-profile.

mind, we now describe and motivate the particular choice of q_0 used for the numerical studies presented in this work.

A. General motivation for considering MHD stability through the lens of continued fractions

Resonances play an essential role in the MHD stability analysis while the difference between a magnetic field line with rational and irrational rotational transform has significant implications in non-axisymmetric equilibria due to the issue of singular currents at rational surfaces.[13,24] The continued fraction representation provides a unified framework for treating both rational and irrational values of q and/or ι. Establishing a connection between key metrics that characterize MHD equilibrium and stability and the structure of real numbers affords access to the mature body of literature knowledge that exists for the generic properties of the real numbers, including convergents and continued fractions, which can then be applied to derive new insights on macroscopic physics properties for magnetically confined plasmas.

Every real number, χ, can be represented as a (simple) continued fraction,[25] where

$$\chi = a_0 + \cfrac{1}{a_1 + \cfrac{1}{a_2 + \cfrac{1}{a_3 + \cfrac{1}{\ddots}}}}, \tag{4}$$

or, more compactly, as $\chi = [a_0; a_1, a_2, a_3, \ldots]$ where $a_{i \geq 0}$ are some integers. A simple continued fraction can be constructed for any $\chi \in \mathbb{R}$ by the following algorithm:[26]

$$
\begin{aligned}
\chi &= a_0 + \xi_0, & 0 \leq \xi_0 < 1, \\
\frac{1}{\xi_0} &= a_1' = a_1 + \xi_1, & 0 \leq \xi_1 < 1, \\
\frac{1}{\xi_1} &= a_2' = a_2 + \xi_2, & 0 \leq \xi_2 < 1, \\
& \quad\vdots,
\end{aligned}
\tag{5}
$$

where $a_{i \geq 0} > 0$ are integers and $a_i = [a_i']$ is the integer component of a_i' with $a_0 = [\chi]$. Note that here we have used the notation $\xi_{i \geq 0}$ to denote the non-integer component of a_i', following the literature convention.[26] This should not be confused with the radial component of the displacement vector, ξ, associated with the MHD stability theory.

If $\xi_N = 0$ for some finite N then (5) terminates and we can write $\chi = [a_0; a_1, \ldots, a_N]$. Otherwise, $\chi = [a_0; a_1, \ldots]$. If a continued fraction terminates at some finite depth, then χ is rational. Otherwise, χ is irrational.

Truncating a continued fraction at some finite depth produces fractions, known as convergents, which are rational approximations of χ that alternate between under- and over-estimating χ. Importantly, each ith convergent, $\chi_i = m_i/n_i = [a_0; a_1, \ldots, a_i]$, is the best rational approximation of χ with denominator less than or equal to n_i.[26] The ith convergent, χ_i, can be calculated from[26]

$$\chi_i = [a_0; , a_1, \ldots, a_i] = \frac{m_i}{n_i} = \frac{a_i m_{i-1} + m_{i-2}}{a_i n_{i-1} + n_{i-2}}, \tag{6}$$

where $(m_0, n_0) = (a_0, 1), (m_1, n_1) = (a_1 a_0 + 1, a_1)$, and $(m_i, n_i) = (a_i m_{i-1} + m_{i-2}, a_i n_{i-1} + n_{i-2})$ for $2 \leq i \leq N$, where $\chi = [a_0; a_1, \ldots, a_N]$.

Formally, when χ is rational such that $\chi = m_k/n_k = [a_0; a_1, \ldots, a_k]$ for some finite k there are two possible continued fraction representations (Theorem 158[26]) since

$$[a_0; a_1, \ldots, a_k] = [a_0; a_1, \ldots, a_k - 1, 1] \quad \text{for } a_k \geq 2, \tag{7}$$

$$[a_0; a_1, \ldots, a_{k-1}, 1] = [a_0; a_1, \ldots, a_{k-1} + 1] \quad \text{for } a_k = 1. \tag{8}$$

By contrast, when χ is irrational, the (infinite) simple continued fraction representation is unique (Theorem 170[26]). If two continued fractions, $[a_0; a_1 \ldots, a_N]$ and $[b_0; b_1 \ldots, b_M]$, have the same sequence of convergents, then the continued fractions are said to be identical.[26] If $[a_0; a_1 \ldots, a_N]$ and $[b_0; b_1 \ldots, b_M]$ have the same value when N and M are finite with $a_N > 1$ and $b_N > 1$, then $N = M$ and the fractions are identical (Theorem 160[26]). Thus, excepting the two cases given by (7) and (8), the sequence of convergents is unique when $\chi \in \mathbb{Q}$. For the exceptional cases, by inspection of (7) and (8) one sees that the penultimate convergent in the sequence will differ depending on the representation (the final one must be identical, by definition). For the irrational case, the sequence is unique. In this work, we focus primarily on the case where χ is irrational since this guarantees uniqueness of the sequence of convergents, in principle. However, in Sec. III C, we will see how practical considerations, such as the fact that q_0 cannot be known or represented exactly, lead to some non-uniqueness irrespective of whether χ is rational or irrational.

The characterization of mode rational surfaces as "low-order" or "high-order" can be an important point of differentiation in the MHD stability literature (see Nührenberg and Zille,[27] for example). The

continued fraction approach provides another quantitative comparison of the characteristics of surfaces in a plasma by examining the number of convergents associated with the continued fraction presentation. For example, consider two mode rational surfaces with $q = m/n$ and $\bar{q} = \bar{m}/\bar{n}$, which can be written as $q = [a_0; a_1, \ldots, a_j]$ and $\bar{q} = [\bar{a}_0; \bar{a}_1, \ldots, \bar{a}_k]$, respectively [cf. Eq. (4)]. Both q and $\bar{q}$ admit a sequence of convergents, of length j and k, respectively. Since q and $\bar{q}$ are rational surfaces, j and k must both be finite. If $j < k$, then the continued fraction representation of q has fewer convergents than $\bar{q}$. This provides a measure of which, if any, other rational surfaces in the vicinity of a resonance are such that the corresponding modes are also likely to be unstable. The language of continued fractions, therefore, presents another way of characterizing individual surfaces and comparing stability properties.

The concept similarly extends to irrational surfaces, where j and k are infinite. In general, as $i \to \infty$, the associated convergent (χ_i) becomes a better absolute approximation of χ, meaning that $|\chi - \chi_i|$ becomes small.[25] Of course, when χ is rational, i is finite, and $|\chi - \chi_i| = 0$ for some i sufficiently large.

For $q \in \mathbb{R}$, we can define

$$\Delta q(m, n) \equiv \left| q - \frac{m}{n} \right|, \tag{9}$$

where $(m, n) \in \mathbb{Z}^2$. An analogous definition can also be constructed for ι. The general study of upper bounds on (9), including for specific choices of n, forms the basis of the theory of Diophantine approximations, and as such, many generic properties are well understood.[26,28] One example is the set of (m, n) corresponding to convergents of q. Thus, for specific choices of (m, n), (9) provides a metric to compare properties such as the "irrationality" of individual surfaces in the plasma (which can be labeled by q or ι). An example application[20] of this general idea is to identify nonresonant modes which are most likely to be unstable. Consider the fact that (9) can be bounded above by $1/\sqrt{5}n^2$. This implies that m/n is a convergent of q (when q is irrational). However, not every convergent satisfies this bound.[26] It has been empirically demonstrated that this property can be used as a necessary condition for identifying the unstable nonresonant pressure-driven MHD modes in some low-shear equilibria.[20]

B. Identifying the mode spectrum

In this work, we are interested in the onset of a linear stability regime dominated by modes associated with convergents of q_0. Hence, we use the properties of convergents to guide the choice of q_0 for the numerical studies presented in Secs. IV and VI. Since the sequence of convergents for q_0 alternates between under- and over-estimating q_0, the associated spectrum contains both resonant and nonresonant modes. Unlike previous work,[20] we consider both the resonant and nonresonant subsets of the mode spectrum.

We seek a choice of q_0 such that the spectrum of modes associated with the low-shear stability regime can be uniquely characterized. Since we consider equilibria relevant to hybrid tokamak scenarios, we consider q_0 close to but above unity. Note that, as $q_0 \to 1$, the numerators and denominators of the associated convergents, q_i, become very large, even for small i. These q_i correspond to modes with large poloidal and toroidal mode numbers, which we expect to be readily stabilized by other effects in practice and, thus, are unimportant in the

stability regime of interest. If q_0 is sufficiently close to one such that only the $q_{i=1}$ convergent is expected to be relevant so far as stability is concerned, then we recover the quasi-interchange regime[16] as $q_{i=1} = 1/1$ in these cases.

As was previously observed,[20] when $q_0 \approx 1.1$ nonresonant modes with intermediate poloidal and toroidal mode numbers can dominate the linear MHD stability properties of the equilibrium if there is no shear in the central plasma volume. Thus, in this work we choose $q_0 \approx 1.3$ and irrational to maximize the number of convergents associated with modes of physically relevant m and n. Next, let us consider the uniqueness of the mode spectrum associated with the convergents of q_0.

C. Non-uniqueness of the q_0 mode spectrum in practice

In practice, one cannot distinguish between whether q_0 is rational or irrational; numerical representations of q_0 are necessarily of finite precision and experimental measurements are limited by finite resolution meaning that measured and derived quantities can only be known with limited precision. Moreover, in an actual experiment, q_0 may also be changing in time. Here, we show that relatively small changes in q_0 can affect the presence of convergents with small denominators and, hence, the predicted mode spectrum. This is true even when the change does not introduce additional low-order rational surfaces into the plasma. In Sec. VI, we will discuss how comparing mode spectra for different values of q can potentially be used to reduce uncertainty when q_0 is obtained experimentally.

For any $q_0 \in \mathbb{R}$, we can construct a sequence of convergents, $(q_i)_{i=1}^k$, where k is finite if q_0 is rational and infinite otherwise. While a sequence, $(q_i)_{i=1}^k$, may be unique for each q_0, a partial sequence, $(q_i)_{i=1}^N$ where $N < k$, may not be, especially if N is small. For example, consider $q_0 = 1.28$ and $q_0 = 1.33$. The latter lies within $\pm 5\%$ of 1.28, which is typical of the accuracy with which q_0 can be determined from experiment.[11] For $q_0 = 1.28$ and $q_0 = 1.33$, we have $(q_i)_{i=1}^{k=4} = (1/1, 4/3, 5/4, 9/7)$ and $(q_i)_{i=1}^{k=2} = (1/1, 4/3)$, respectively. Note that $q_{i,\text{odd}}$ and $q_{i,\text{even}}$ are, respectively, associated with nonresonant and resonant modes. The partial sequences, $(q_i)_{i=1}^N$, for $q_0 = 1.28$ and $q_0 = 1.33$, are identical for $N \leq 2$. Consequently, the associated mode spectra will be indistinguishable up to $n = 3$. However, in a low-shear regime where nonresonant modes become unstable, we would expect to see an $(m = 5, n = 4)$ mode if $q_0 = 1.28$ but not if $q_0 = 1.33$, giving rise to a characteristic mode spectrum that differentiates $q_0 = 1.28$ from $q_0 = 1.33$. Moreover, if nonresonant modes dominate the plasma stability properties when shear is reduced, we would expect to observe a clear transition to mode spectra determined by the sequence $(q_i)_{i=1}^k$, for sufficiently low shear. Applied to the example considered above, the transition to a low shear MHD stability regime for $q_0 = 1.28$ would be characterized by the preferential destabilization of the (nonresonant) $(m = 5, n = 4)$ mode over the (resonant) $(m = 6, n = 4)$ mode or any other mode with $m > 6$ and $n = 4$. Therefore, tracking the poloidal mode number of the dominant instability for each n in the expected mode spectrum associated with q_0 provides a straightforward way to identify the onset of the low-shear MHD stability regime. As will be seen in Sec. IV, there is a clear correlation between shear and stability of these modes.
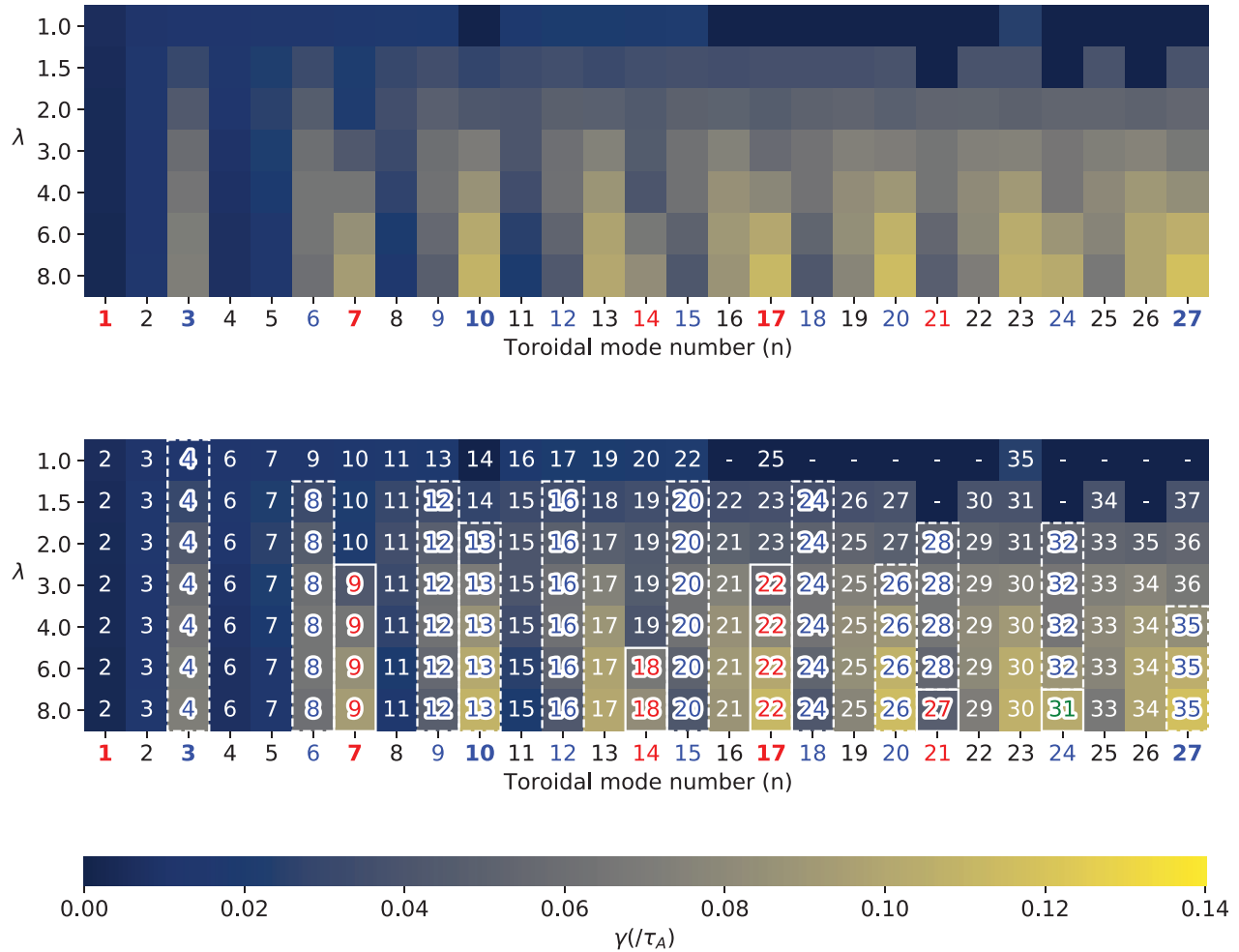
FIG. 2. (Top) The spectrum of non-ideal linear growth rates, $\gamma(n)$, for $1 \leq n \leq 27$, computed using M3D-C[1] for each equilibrium profile given by (1) and (2) with $1 \leq \lambda \leq 8$. Here, increasing λ corresponds to decreasing shear. Blue (dashed box) and red (solid box) labels, respectively, denote modes in the resonant and nonresonant subsets of the spectrum associated with q_0, see (11). Modes associated with the fundamental harmonics are shown in bold on the horizontal axis. (Bottom) For each (n, λ), the poloidal mode number of the fastest-growing mode is indicated. All other modes correspond to resonant instabilities not in the spectrum of q_0.

D. Choice of q_0

In view of the additional stabilization effects previously alluded to, in practice mode spectra corresponding to different q_0 are differentiable only if the partial sequences, $(q_i)_{i=1}^{N}$, become distinguishable for some N not too large. Specifically, the poloidal and toroidal mode numbers of the mode associated with q_N must be less than the maximum resolvable resolution, whether experimental or numerical. Otherwise, the q_0s are effectively same.

For this work, we choose $q_0(x_1 = 4, x_2 = 9, x_3 = 3, x_4 = 7)$ $\approx 1.295\,69$ where

$$q_0(x_1, x_2, x_3, x_4) = \frac{x_1 + x_2\phi}{x_3 + x_4\phi}, \tag{10}$$

with $\phi = (\sqrt{5} + 1)/2$ and such that $q_0(x_1, x_2, x_3, x_4) \in \mathbb{R}\backslash\mathbb{Q}$. The mode spectrum associated with $(q_i)_{i=1}^{N=6}$ (up to $n \leq 27$) for q_0 is

$$(q_i)_{i=1}^{N=6} : (1,1), (4,3), (9,7), (13,10), (22,17), (35,27). \tag{11}$$

This particular value of q_0 was chosen for the present study because of the comparatively large number of low- and moderate-n modes in the spectrum associated with the sequence of convergents, $(q_i)_{i=1}^{k}$. We emphasize that the approach is applicable to both rational and irrational q_0.

Starting from $(1,1)$, modes in the q_0 mode spectrum in Eq. (11) alternate between being nonresonant and resonant. As the shear is reduced, we define the onset of the low-shear nonresonant MHD stability regime to be characterized by preferential destabilization of these modes, over any other resonant instabilities with the same toroidal mode number for $n > 1$. The modes shown in (11) correspond to the fundamental harmonics associated with each convergent of q_0. However, that is not to say that higher-order harmonics, e.g., the $(m = 8, n = 6)$ and $(m = 12, n = 9)$ modes etc., are expected to be
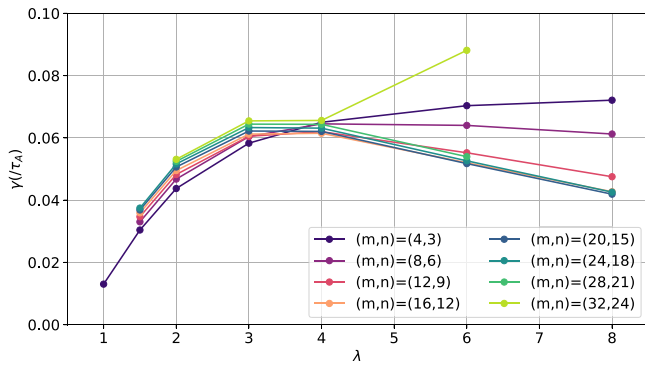
FIG. 3. Non-ideal linear growth rates of the $(m = 4, n = 3)$ mode and its higher-order harmonics up to $n = 24$. The $(m = 4, n = 3)$ mode is part of the resonant subset of the mode spectrum associated with q_0.

stable. Indeed, in Sec. V we show that, in the low-shear stability regime, modes corresponding to higher-order harmonics of the spectrum are also preferentially destabilized.

IV. ONSET OF NONRESONANT MODES WITH REDUCED SHEAR

For $q_0 \approx 1.295\,69$, we compute the spectrum of the non-ideal linear growth rate, γ, as a function of toroidal mode number with $1 \leq n \leq 27$, for each equilibrium profile given by (1) and (2) with $1 \leq \lambda \leq 8$. The non-ideal growth rate spectrum is presented in Fig. 2 and accompanied by an annotated breakdown of the fastest-growing linearly unstable mode for each n. The non-ideal growth rates are calculated by using the initial-value extended-MHD code, M3D-C[1], to solve linearized non-ideal single-fluid dissipative MHD equations with isotropic transport parameters.[22] For each prescribed toroidal mode number, the linear growth rate corresponds to that of the fastest growing (m, n) mode. The thermal conductivity model is given by

$$\mathbf{q} = -\kappa_t \nabla T, \tag{12}$$

where $T = T_e + T_i$, and T_e and T_i are the electron and ion temperatures, respectively. We choose isotropic values of resistivity and viscosity, such that $P_m \equiv \nu/\eta = 10^{-1}$, $S = 4.6 \times 10^5$, and $\kappa_t = 1$ W/mK, where P_m and S are, respectively, the magnetic Prandtl number and Lundquist number. The decision to use M3D-C[1] for this work was motivated by the study of nonlinear stability, which is the subject of the on-going work. For a standalone analysis of linear stability, a dedicated eigenvalue solver such as DCON[29] would be similarly well-suited.

Recalling that increasing λ corresponds to decreasing shear, in Fig. 2 we observe a clear transition to a linear MHD stability regime, which is dominated by the mode spectrum associated with convergents of q_0. In particular, for $\lambda \geq 3$ (which corresponds to the low-shear region extending to $x \approx 0.4$), the mode spectrum develops a distinctive vertical striation pattern. The vertical striping is reminiscent of the observed behavior for infernal modes[21] and consistent with a case considered previously[20] where the plasma is shear free in the core and all resonances excluded.

For each (n, λ) pair, the poloidal mode number of the fastest-growing non-ideal linear instability, as calculated by M3D-C[1], is also labeled in Fig. 2. Resonant and nonresonant modes corresponding to the spectrum associated with q_0 are colored blue and red, respectively. Modes associated with the fundamental harmonics are shown in bold. All other modes correspond to resonant instabilities not in the spectrum associated with q_0.

As expected, we find that the nonresonant $(m = 1, n = 1)$ mode is subdominant to the resonant $(m = 2, n = 1)$ mode, which is only weakly unstable for all values of λ considered. As observed previously,[10,20] the nonresonant $(m = 1, n = 1)$ mode is not expected to be destabilized until $q_0 \lesssim 1.05$, whereas $q_0 \approx 1.3$ in the present case.

The $(m = 4, n = 3)$ mode forms part of the resonant subset of the mode spectrum associated with q_0, and we find that it is unstable, albeit comparatively weakly, for all values of λ considered. Moreover, a large number of modes corresponding to higher order harmonics of 4/3 are destabilized at moderate values of shear where $\lambda \geq 1.5$. For $\lambda \geq 1.5$, up to 7 harmonics of 4/3 are destabilized, in addition to the $(m = 4, n = 3)$ mode. As can be seen in Fig. 3, the growth rates of the higher order harmonics are comparable to that of the $(m = 4, n = 3)$ mode, especially for $1.5 \leq \lambda \leq 4$. Similar behavior is observed for the $(m = 13, n = 10)$ mode, which is also in the resonant subset of the mode spectrum associated with q_0.

In Fig. 4, we plot profiles of the linearly perturbed pressure, p, and toroidal current density, J_φ, for $\lambda = 8$, which are illustrative of what is observed in Fig. 3. In Fig. 5, we plot the accompanying radial magnetic field for these three modes. Since we are solving the linearized extended-MHD evolution equations, the magnitudes associated with the profiles in Fig. 4 are unimportant; eventually, the system will be dominated by the evolution of the fastest-growing linear instability, which grows exponentially in time. We remark that our purpose here is not to provide a comprehensive classification of the different ideal and resistive modes that comprise the spectra in Fig. 2. Instead, the motivation and focus of this work is to consider the overarching characteristics of the spectrum and its connection to rational approximations of q_0. We now discuss some qualitative features of the profiles.

Profiles for the $(m = 3, n = 2)$ mode are as expected of a standard resonant, internal mode. Namely, the variation in pressure vanishes sharply at the resonant surface (indicated in Fig. 4 by the solid red line), as does the radial component of **B**. The current density profile is strongly localized about the mode rational surface ($q = 3/2$ in this case) and displays current-sheet-like characteristics. From Fig. 5, the notable feature of the nonresonant $(m = 9, n = 7)$ mode is that the radial mode structure does not vanish. Moreover, the spatial variation of both J_φ and p coincide, albeit with opposite polarity. Unlike the resonant $(m = 13, n = 10)$ mode, which exhibits a similarly extended pressure profile or the $(m = 3, n = 2)$ mode, the current density cannot be localized to a resonant surface (as there is none), yielding a different structure. For the resonant $(m = 13, n = 10)$ mode, we observe some localization of J_φ about the $q = 13/10$ resonant surface that is reminiscent of the current-sheet-like structures seen for the $(m = 3, n = 2)$ mode. However, unlike the resonant $(m = 3, n = 2)$ mode, localization of the pressure perturbation is not strongly correlated with the mode rational surface. Like the $(m = 3, n = 2)$ mode, we also find that $|B_r|$ sharply decreases toward zero in the vicinity of the $q = 13/10$ surface, as expected of a resonant instability. We observe similar behavior for other (resonant) higher-n modes that are not part of the q_0 spectrum.
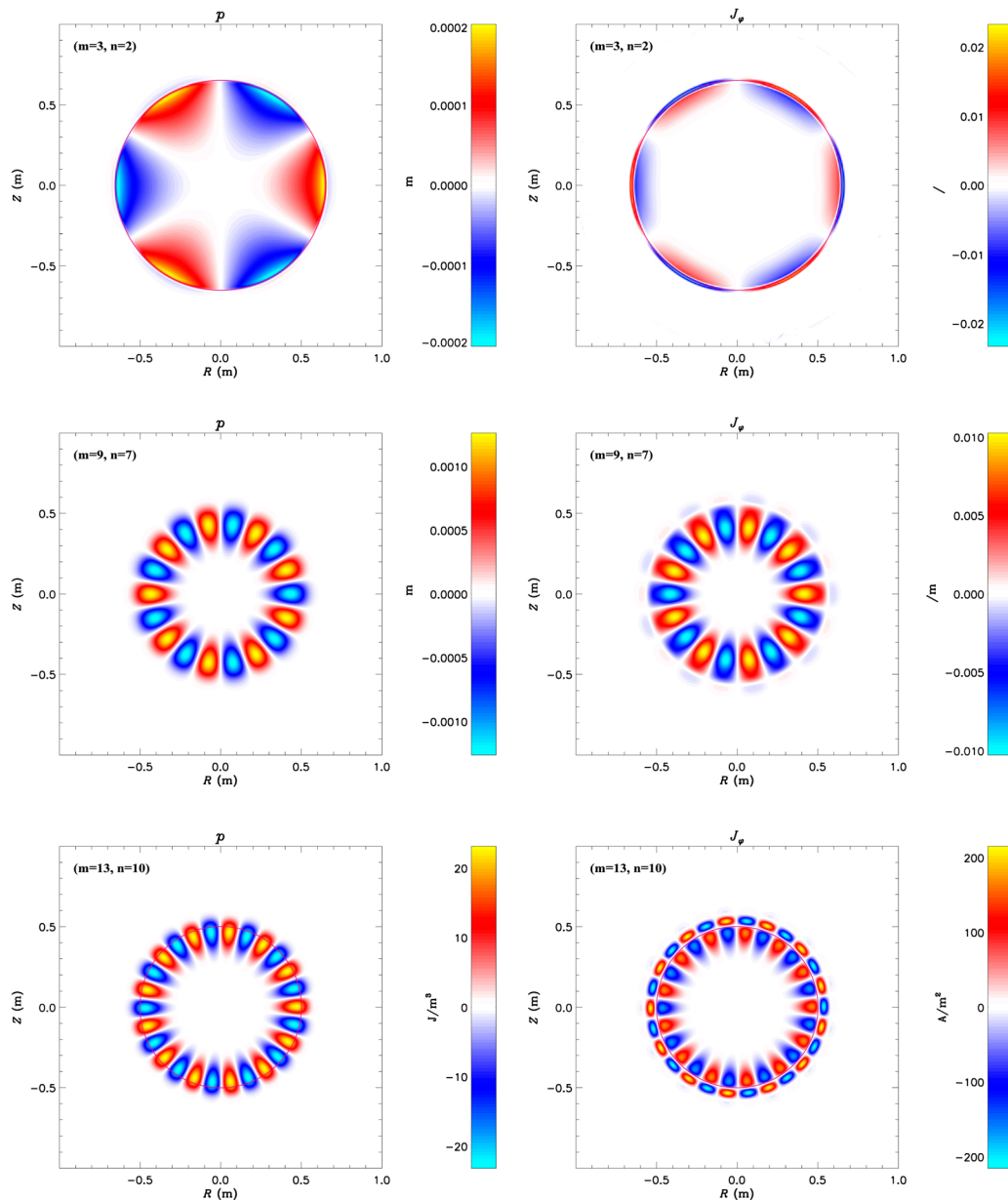
FIG. 4. Profiles of the linearly perturbed pressure, p, (left) and toroidal current density, J_φ, (right) for the $(m = 3, n = 2)$ (top), $(m = 9, n = 7)$ (middle), and $(m = 13, n = 10)$ modes (bottom) with $\lambda = 8$. These are representative of the three types of profiles observed in Fig. 2.

V. PREFERENTIAL DESTABILISATION OF NONRESONANT MODES

In Sec. III, we defined the onset of the low-shear nonresonant MHD stability regime as being characterized by preferential desta-bilization of modes in the spectrum associated with the sequence of convergents, $(q_i)_{i=1}^k$, for q_0 over any other resonant instabilities with the same toroidal mode number when $n > 1$. As was clearly seen in Fig. 2 and discussed in Sec. IV, for $\lambda \geq 3$ (which

corresponds to the low-shear region extending to $x \approx 0.4$ and beyond), both resonant and nonresonant modes in the spectrum associated with q_0 are destabilized, grow robustly and come to dominate the overall linear stability MHD properties of the equi-librium for $\lambda \geq 4$. This behavior is quantitatively illustrated in Fig. 6, where we plot non-ideal growth rates of the fastest-growing for each n corresponding to a denominator in the partial sequence of convergents, $(q_i)_{i=1}^{N=5}$, for q_0. Growth rates of modes with poloidal
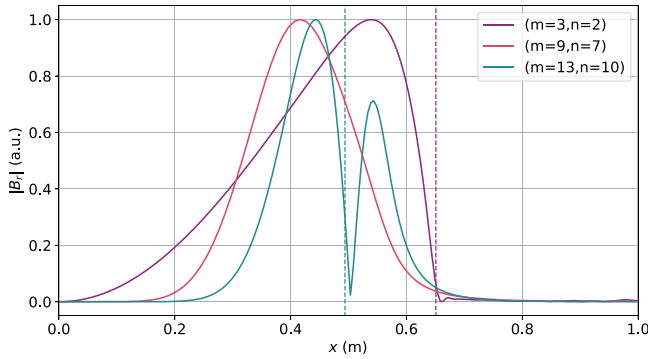
FIG. 5. Profiles of the radial magnetic field for the $(m = 3, n = 2)$ (purple), $(m = 9, n = 7)$ (pink), and $(m = 13, n = 10)$ (teal) modes for $\lambda = 8$. The $(m = 9, n = 7)$ mode structure is globally extended and characteristic of nonresonant modes. By contrast, since both the $(m = 3, n = 2)$ and $(m = 13, n = 10)$ modes are resonant, B_r changes sign near the mode rational surface. The corresponding resonant surfaces (dashed lines) are located at $x = 0.494$ and $x = 0.651$, respectively.
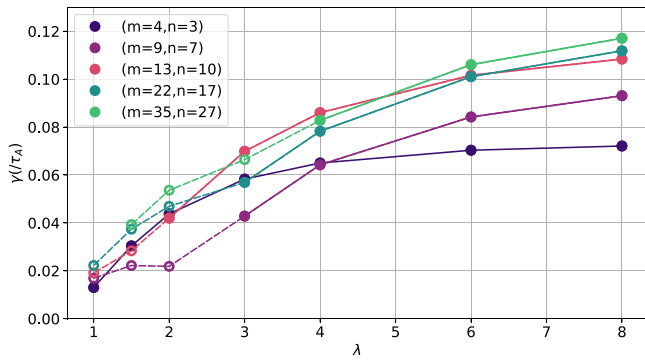

FIG. 6. Non-ideal linear growth rates of both resonant and nonresonant modes in the spectrum associated with q_0. Cases where the fastest-growing instability with the given n does not correspond to modes in the spectrum associated with q_0 are denoted by open circles.
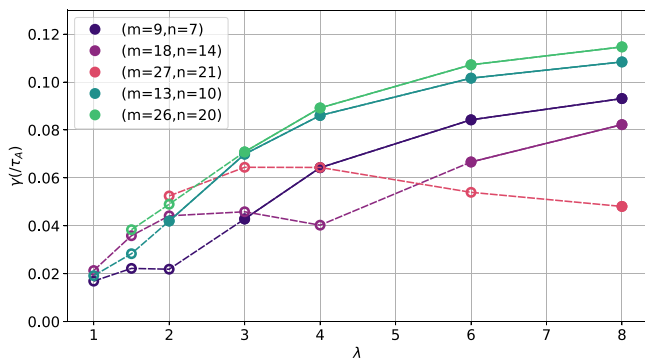

FIG. 7. Non-ideal linear growth rates of the $(m = 9, n = 7)$ and $(m = 13, n = 10)$ modes and higher-order harmonics up to $n = 27$, which are, respectively, members of the nonresonant and resonant subsets of the spectrum associated with q_0. Cases where the fastest-growing instability with the given n does not correspond to modes in the spectrum associated with q_0 are denoted by open circles.

mode number, m, which correspond to the numerator of each term in $(q_i)_{i=1}^{N=5}$, are denoted by filled circles. Hollow circles indicate modes with poloidal mode number such that $m \neq nq_i$.

For the reference case, $\lambda = 1$, the q-profile is quadratic in the radial coordinate. In this case, of the modes in the spectrum associated with q_0, only the (resonant) $(m = 4, n = 3)$ mode is unstable and very weakly so. As the shear is decreased, we observe a steady increase in γ, in addition to destabilization of all modes in the spectrum associated with q_0.

In Fig. 6, we considered growth rates of the fundamental harmonics of the mode spectrum for q_0, whereas in Fig. 7, we compare γ of both the fundamental and higher order harmonics of the fastest-growing modes with $n = 7, 14$, and 21 as well as $n = 10$ and 20. These are, respectively, associated with the harmonics of the nonresonant $(m = 9, n = 7)$ and resonant $(m = 13, n = 10)$ modes that partially comprise the spectrum associated with q_0. Like Fig. 6, we observe an overall increase in γ with the decreasing shear (i.e., increasing λ).

For $\lambda = 8$, the low-shear region extends to $x \approx 0.55$, which is the maximum value considered in this study. Interestingly, in Fig. 2, we observe that for $(n = 21, \lambda = 8)$, the fastest growing linear instability does not correspond to a higher-order harmonic of the $(m = 4, n = 3)$ mode, as is the case for $\lambda \leq 6$. Instead, the fastest-growing instability is the $(m = 27, n = 21)$ mode, which is a higher-order harmonic of the $(m = 9, n = 7)$ mode and part of the subset of nonresonant modes associated with q_0. This suggests that, at sufficiently low shear ($\lambda = 8$ in this case), there is preferential destabilization of higher-order harmonics in the nonresonant subset of the q_0 spectrum.

Taken together, Figs. 3, 6, and 7 indicate that both fundamental and higher order harmonics of modes in the nonresonant subset of the mode spectrum associated with q_0 are preferentially destabilized as magnetic shear is reduced. Even up to relatively high n, the higher-order harmonics can have non-ideal linear growth rates that are comparable to those of the fundamental harmonic. Combined these modes have a potentially defining impact on the MHD stability characteristics in the low-shear regime.

VI. EFFECT OF OTHER NONRESONANT MODES ON THE LOW-SHEAR MHD STABILITY REGIME

In this final section, we consider an apparently anomalous observation in Fig. 2, which is that the $(m = 31, n = 24)$ mode is the dominant linear instability with $n = 24$ when $\lambda = 8$. We then propose an approach that can be potentially applied to reduce the uncertainty on q_0 obtained via measurement or through equilibrium reconstruction, based on the fact that each q can be associated with a mode spectrum that is (almost) unique (cf. Sec. III C).

For $\lambda \leq 6$, the dominant linear instability with $n = 24$ is the $(m = 28, n = 24)$ mode, which is a higher-order harmonic of the $(m = 4, n = 3)$ mode and a member of the resonant subset of the q_0 spectrum. When $\lambda = 8$, it is the $(m = 31, n = 24)$ mode which dominates instead. However, $31/24$ is not a convergent of q_0. Since $31/24 = 1.29167 < q_0$, the $(m = 31, n = 24)$ mode is nonresonant. Clearly, at sufficiently weak shear additional nonresonant modes are destabilized. To differentiate between nonresonant modes which are associated and are not associated with convergents of q_0, we refer to the latter as "other nonresonant" modes.
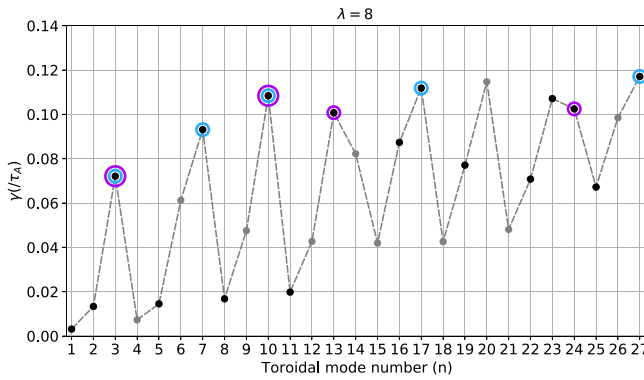
FIG. 8. The non-ideal linear growth rate spectrum (up to $n = 27$) for $\lambda = 8$ calculated used M3D-C[1]. The growth rates corresponding to the fundamental and higher-order harmonics of the unstable modes are shaded black and gray, respectively. The fundamental harmonics of modes in the spectrum associated with $\chi' \approx 1.295\,69$ and $\chi \approx 1.305\,21$ are highlighted in blue and purple, respectively.

Figure 2 suggests that the effect of other resonant modes on the overall MHD stability characteristics is subdominant to modes in the spectrum associated with q_0. Nonetheless, it can be useful to determine which other resonant modes are likely to be destabilized when the shear is sufficiently weak. To do so requires being able to determine the real numbers with which the other nonresonant modes are associated. A preliminary step is to identify an interval, $\Delta\chi \subset \mathbb{R}$, where the mode/s of interest correspond to convergents of $\chi \in \Delta\chi$. The development of a formal procedure for doing so is the subject of on-going work so we briefly sketch one practical approach.

For the particular case at hand, we empirically determine that 31/24 is a convergent of some χ in $\Delta\chi = (1.289\,96, 1.292\,35]$. Specifically, for 10^6 pseudorandom numbers between $0.6 < \chi < 2$, we compute the first eight convergents of each χ to determine the approximate $\Delta\chi$ such that 31/24 is a convergent of χ. The range of test values is centered about q_0 and extends up to 2 which, as can be seen from Fig. 1, includes q-values that are resonant well into the strongly sheared region. Importantly, we remark that the choice of $\Delta\chi$ is not unique. Indeed, one may observe that $\Delta\chi = [1.290\,33, 1.292\,68]$ is also a valid choice (as it contains 31/24 as a convergent) and use the corresponding $\Delta\chi$ as a starting point for further analysis instead. (Since the actual value of q_0 is known, the example is somewhat contrived. Nonetheless, it illustrates how the general principle can be applied.)

Proceeding as described in Sec. III D, for a range of different trial values, $\chi \in \Delta\chi$, we can then construct mode spectra based on the sequence of convergents for each χ. Modes in the spectrum associated with q_0 alternate between being nonresonant and resonant. By contrast, depending on whether $\chi < q_0$ or $\chi > q_0$, the spectrum associated with χ may consist of all, none, or some nonresonant modes that do not necessarily alternate between being nonresonant and resonant. Moreover, if $|q_0 - \chi|$ is sufficiently small, then the sequences of convergents, $(\chi_i)_{i=1}^M$ and $(q_{0,i})_{i=1}^N$, may have many common elements on account of the non-uniqueness discussed in Sec. III C. Even so, by comparing the characteristics of each spectrum and the expected properties of the associated unstable modes, it can be possible to determine which mode spectrum is dominant. As will be discussed, a similar procedure

can potentially be applied to reduce uncertainty on q_0 by analyzing the mode spectra associated with a range of trial values and comparing against observation to determine the best fit.

As an example, consider the trial value $\chi = \pi^3/24 \approx 1.291\,93$, which is in the interval $\Delta\chi$ and associated with the partial sequence of convergents given by

$$(\chi_i)_{i=1}^{N=6} = \left(\frac{1}{1}, \frac{4}{3}, \frac{9}{7}, \frac{22}{17}, \frac{31}{24}, \frac{177}{137}\right). \tag{13}$$

We note that $\chi < q_0$. Comparing to (11), we can see that the partial sequence of convergents for q_0 and χ is nearly identical for $N \leq 5$. Namely, $(\chi_i)_{i=1}^{N=5}$ includes 31/24 but not 13/10 and vice versa for $(q_{0,i})_{i=1}^{N=5}$. From Fig. 2 and as noted in Sec. IV, the $(m = 13, n = 10)$ mode is dominant at moderate shear ($\lambda = 2$), as are the other modes in the spectrum associated with q_0. We can, therefore, conclude that modes in spectrum associated with χ are subdominant compared to q_0 because modes in the spectrum associated with χ do not become the fastest-growing linear instability (for a given n) until the shear is very weak.

A. Reducing uncertainty on q_0

At first glance, the preceding example may appear trivial since q_0 is known in this case. However, we now illustrate how the same logic may be applied when q_0 is not known exactly. We propose that this idea could, in principle, be used to reduce uncertainty on q_0 obtained via measurement or through equilibrium reconstruction. First, we give a worked example using the results in hand as a proof-of-principle for how this might be applied in practice. We then address the generalization of this approach, which is presently under development and aims to set these ideas on firmer footing.

Suppose we know that q_0 lies in some interval, $\Delta\chi$, but the exact value is unknown. We pick some trial values in $\Delta\chi$, for example, $\chi' = (4 + 9\phi)/(3 + 7\phi) \approx 1.295\,69$ and $\chi = (9 + 4\phi)/(7 + 3\phi) \approx 1.305\,21$ so that $\{\chi, \chi'\} \in \Delta\chi$. For each χ' and χ, we construct the associated mode spectrum from the sequence of convergents given by

$$(\chi_i')_{i=1}^{N'} = \frac{1}{1}, \frac{4}{3}, \frac{9}{7}, \frac{13}{10}, \frac{22}{17}, \frac{35}{27}, \tag{14}$$

$$(\chi_i)_{i=1}^{N} = \frac{1}{1}, \frac{4}{3}, \frac{13}{10}, \frac{17}{13}, \frac{30}{23}, \frac{47}{36}, \tag{15}$$

where, as in (11), starting from 1/1 modes in the spectra alternate between being nonresonant and resonant.

Next, suppose we have some knowledge of the unstable mode spectrum of the equilibrium. As an example, we consider Fig. 8, which is the $\lambda = 8$ case of Fig. 2. We begin by analyzing Fig. 8 and identifying the fundamental harmonics of all the unstable modes. The subsets of modes in the spectra associated with χ' and χ are highlighted in blue and purple, respectively. We see that the $(m = 9, n = 7)$, $(m = 22, n = 17)$ and $(m = 35, n = 27)$ modes are unique to the spectrum associated with χ', whereas the $(m = 17, n = 13)$ and $(m = 30, n = 23)$ modes are unique to χ.

We now wish to reduce the uncertainty on q_0 by reducing the size of $\Delta\chi$. Note that all modes (up to $n = 27$) associated with the spectra of χ and χ' are unstable for $\lambda = 8$. In fact, from Fig. 2 we see that the modes associated with both χ and χ' are all destabilized at moderately low shear, $\lambda \approx 4$. We, therefore, cannot use one mode spectrum

being subdominant to another as a means to constrain q_0, as was the case for (13). Instead, we can examine the structure of individual modes. Specifically, we consider the $(m = 9, n = 7)$ mode. As discussed in Sec. IV, the profiles associated with the $(m = 9, n = 7)$ mode are clearly indicative of a nonresonant instability. Having deduced that the $(m = 9, n = 7)$ mode is nonresonant, the implication is that $9/7 < \chi'$ and $9/7 < \min(\Delta\chi)$. This constrains q_0 by reducing the interval, $\Delta\chi$.

The generalization of this approach to one that is systematic relies on using what is known about the sequence of convergents associated with a given real number, to judiciously guide the choice of the trial values, χ. One approach, currently under development, is to select χs from a particular equivalence class of irrational numbers, based on the quantity of elements in the corresponding sequence of convergents which have a denominator that is not too large (and can be feasibly measured in experiment). Consider two numbers, $\chi_1, \chi_2 \in \mathbb{R}$. Here, χ_2 is said to be equivalent to χ_1 if

$$\chi_2 = \frac{a'\chi_1 + b'}{c'\chi_1 + d'}, \tag{16}$$

where a', b', c', and d' are integers such that $a'd' - b'c' = \pm 1$.[26] For example, one could pick χs that are equivalent [in the sense of (16)] to ϕ, the Golden Mean, which has the property of having many convergents with relatively small denominators. This was seen in the previous work[20] where the q_0 values considered were all equivalent to ϕ. Hence, the nonresonant mode spectrum for each case contained multiple low-/moderate-n modes. The natural limitation of this approach is its dependence on the distribution of equivalent numbers in $\mathbb{R}$, which consequently means that the trial values do not uniformly sample the subset $\mathbb{R}$ spanned by q.

The degree to which this approach can potentially reduce the uncertainty on q_0 depends on details of the problem under consideration. Moreover, since this approach relies on being in the low shear regime, a method to explicitly connect the mode spectrum with the shear parameter is needed. However, the potential utility in applications, such as equilibrium reconstruction, justifies continued development, as is the subject of the on-going work. In many circumstances, the calculated MHD stability properties sensitively depend on the choice of q_0, ι_0, or other extremal values of q and ι (the sawtooth phenomenon being an obvious example). Accurate reconstruction of these values is, therefore, of great importance.

VII. CONCLUSIONS

Equilibria with extended regions of weak magnetic shear, as encountered in hybrid tokamak scenarios and stellarators, can be susceptible to pressure-driven internal MHD modes that would otherwise be stabilized magnetic shear. In particular, nonresonant modes—that is, modes with poloidal and toroidal mode number m and n such that there is no mode rational surface ($q = m/n$) in the plasma—can become key determinants of the overall equilibrium MHD stability properties. Since nonresonant modes can have properties that are unattractive for confinement, including displacing substantial volumes of the plasma and leading to more efficient pressure gradient flattening in the nonlinear regime, the ability to understand and predict the spectrum of unstable nonresonant and "nearly resonant" modes is important.

In Sec. III, we discussed how the continued fraction representation provides a unified framework for treating rational and irrational values of q and ι and, by extension, a pathway to connecting what is well-established about the structure of numbers to plasma properties in MHD. Specifically, we described how the partial sequence of convergents $(q_i)_{i=1}^{N}$ associated with a q-value (or, analogously, ι-value) of interest can be used to predict a spectrum of resonant and nonresonant modes that turn out to be well correlated with the spectrum of unstable MHD modes in configurations with extended regions of weak magnetic shear. In low-shear regimes, each q_0 can be associated with a characteristic mode spectrum that is unique (with two exceptions), in principle. Comparing the unstable modes observed in experiment to the predicted mode spectrum provides a potentially straightforward way to reduce the uncertainty on q_0 obtained via measurement or through equilibrium reconstruction.

In Sec. IV, we explored the onset of nonresonant modes with decreasing shear, for a sequence of equilibria with a fixed value of q_0. The particular q_0 was chosen for the number of low- and moderate-n modes in the spectrum associated with the corresponding sequence of convergents, $(q_i)_{i=1}^{N=6}$. We defined onset of the low-shear nonresonant MHD stability regime as being characterized by the preferential destabilization of nonresonant modes associated with the spectrum of q_0, over any other resonant instabilities with the same toroidal mode number when $n > 1$. Using the initial-value extended-MHD code, M3D-C[1], we computed the spectrum of non-ideal linear growth rates as a function of toroidal mode number for $1 \leq n \leq 27$.

As the shear is reduced, we observed a clear transition to a linear MHD stability regime dominated by resonant and nonresonant modes in the spectrum associated with convergents of q_0. Moreover, we showed that both resonant and nonresonant modes in the spectrum associated with q_0 can be destabilized and grow robustly. This indicates that tracking the poloidal mode number of the dominant instability for each n in the spectrum associated with q_0 provides a straightforward way to identify the onset of the low-shear MHD stability regime. Since there is a clear correlation between shear and the stability of these modes, it is possible that this approach can be used to reduce the uncertainty on shear in the core region, in the analysis and reconstruction of experimental results.

In Sec. V, we observed that, as the region of weak magnetic shear is extended, both the fundamental and higher-order harmonics of modes in the nonresonant subset of the q_0 spectrum are destabilized preferentially to any other resonant instability with the same toroidal mode number with $n > 1$. Even up to relatively high-n, we found that the higher-order harmonics can have non-ideal linear growth rates which are comparable to those of the fundamental harmonic.

In Sec. VI, we considered "other nonresonant modes," which are nonresonant modes not contained in the mode spectrum associated with q_0. These modes were shown to be destabilized with sufficiently weak shear and have a subdominant effect on the overall stability properties of the equilibrium. Since each real number can be associated with a characteristic mode spectrum, we then proposed a procedure that may potentially be applied to reduce the uncertainty on q_0. Additional developments required to realize this for experimental applications were also considered. Since calculated MHD stability properties depend sensitively on the choice of q_0, ι_0, or other extremal values of q and ι, accurate reconstruction of these values is important in many fusion applications.

Even with complete suppression of poloidal and toroidal coupling as a potential source of instability drive, we have seen that equilibria with extended regions of weak magnetic shear can exhibit a broad range of linear MHD instabilities. Importantly, nonresonant modes, as considered in this work, can play a marked role in determining the overall MHD stability properties of equilibria with weak magnetic shear. While the introduction of mode coupling necessarily complicates the analysis, we posit that the effects discussed in this work persist since they relate to the intrinsic structure of numbers and the nature of resonances, which remain unchanged in toroidal geometry. Ultimately, it is the magnetic shear stabilization which enables nonresonant and "nearly resonant" modes to be important from the physics point-of-view. Thus, the pertinent question is to what degree the reduction in magnetic shear stabilization is a dominant contributor to the overall equilibrium stability characteristics in more realistic geometries. In a scenario where such an effect is indeed important, one would expect additional modes to be destabilized through coupling to the resonant and nonresonant modes described in this work. Since the coupling effects are well-understood, e.g., $m \pm 1$ in tokamaks and toroidal "mode families" in stellarators, it should be possible to predict, to a large extent, the spectrum of excited modes by an analysis of the q- or ι-profile, using continued fractions and the approach described in this work. An exploration of these ideas is the basis of ongoing work.

ACKNOWLEDGMENTS

DATA AVAILABILITY

The data that support the findings of this study are available from the corresponding author upon reasonable request.

REFERENCES

[1] T. Tatsuno, M. Wakatani, and K. Ichiguchi, "Ideal interchange instabilities in stellarators with a magnetic hill," Nucl. Fusion **39**(10), 1391 (1999).

[2] G. Y. Fu, W. A. Cooper, R. Gruber, U. Schwenn, and D. V. Anderson, "Fully three-dimensional ideal magnetohydrodynamic stability analysis of low-n modes and Mercier modes in stellarators," Phys. Fluids B **4**(6), 1401–1411 (1992).

[3] C. Gormezano, A. C. C. Sips, T. C. Luce, S. Ide, A. Becoulet, X. Litaudon, A. Isayama, J. Hobirk, M. R. Wade, T. Oikawa, R. Prater, A. Zvonkov, B. Lloyd, T. Suzuki, E. Barbato, P. Bonoli, C. K. Phillips, V. Vdovin, E. Joffrin, T. Casper, J. Ferron, D. Mazon, D. Moreau, R. Bundy, C. Kessel, A. Fukuyama, N. Hayashi, F. Imbeaux, M. Murakami, A. R. Polevoi, and H. E. St John, "Chapter 6: Steady state operation," Nucl. Fusion **47**(6), S285–S336 (2007).

[4] I. T. Chapman, M.-D. Hua, S. D. Pinches, R. J. Akers, A. R. Field, J. P. Graves, R. J. Hastie, C. A. Michael, and MAST Team, "Saturated ideal modes in advanced tokamak regimes in MAST," Nucl. Fusion **50**(4), 045007 (2010).

[5] D. Brunetti, J. P. Graves, W. A. Cooper, and C. Wahlberg, "Fast growing resistive two fluid instabilities in hybrid-like tokamak configuration," Plasma Phys. Controlled Fusion **56**(7), 075025 (2014).

[6] C. J. Ham, J. W. Connor, S. C. Cowley, C. G. Gimblett, R. J. Hastie, T. C. Hender, and T. J. Martin, "Strong toroidal effects on tokamak tearing mode stability in the hybrid and conventional scenarios," Plasma Phys. Controlled Fusion **54**(2), 025009 (2012).

[7] S. G. Lee, J. Seol, H. H. Lee, A. Y. Aydemir, L. Terzolo, K. D. Lee, Y. S. Bae, J. G. Bak, G. H. Choe, G. S. Yun et al., "Long-lived pressure-driven coherent structures in KSTAR plasmas," Phys. Plasmas **23**(5), 052511 (2016).

[8] W. A. Cooper, I. T. Chapman, O. Schmitz, A. D. Turnbull, B. J. Tobias, E. A. Lazarus, F. Turco, M. J. Lanctot, T. E. Evans, J. P. Graves et al., "Bifurcated helical core equilibrium states in tokamaks," Nucl. Fusion **53**(7), 073021 (2013).

[9] J. A. Wesson, "Sawtooth oscillations," Plasma Phys. Controlled Fusion **28**(1A), 243 (1986).

[10] K. Kirby, "Numerical simulations of ideal internal kink modes with flat central q-profile," Nucl. Fusion **28**(2), 231 (1988).

[11] S. C. Jardin, I. Krebs, and N. Ferraro, "A new explanation of the sawtooth phenomena in tokamaks," Phys. Plasmas **27**(3), 032509 (2020).

[12] R. J. Hastie, "Sawtooth instability in tokamak plasmas," Astrophys. Space Sci. **256**(1–2), 177–204 (1997).

[13] L.-M. Imbert-Gerard, E. J. Paul, and A. M. Wright, "An introduction to stellarators: From magnetic fields to symmetries and optimization," arXiv:1908.05360 (2020).

[14] R. C. Wolf, A. Alonso, S. Äkäslompolo, J. Baldzuhn, M. Beurskens, C. D. Beidler, C. Biedermann, H.-S. Bosch, S. Bozhenkov, R. Brakel, H. Braune, S. Brezinsek, K.-J. Brunner, H. Damm, A. Dinklage, P. Drewelow, F. Effenberg, Y. Feng, O. Ford, G. Fuchert, Y. Gao, J. Geiger, O. Grulke, N. Harder, D. Hartmann, P. Helander, B. Heinemann, M. Hirsch, U. Höfel, C. Hopf, K. Ida, M. Isobe, M. W. Jakubowski, Y. O. Kazakov, C. Killer, T. Klinger, J. Knauer, R. König, M. Krychowiak, A. Langenberg, H. P. Laqua, S. Lazerson, P. McNeely, S. Marsen, N. Marushchenko, R. Nocentini, K. Ogawa, G. Orozco, M. Osakabe, M. Otte, N. Pablant, E. Pasch, A. Pavone, M. Porkolab, A. Puig Sitjes, K. Rahbarnia, R. Riedl, N. Rust, E. Scott, J. Schilling, R. Schroeder, T. Stange, A. von Stechow, E. Strumberger, T. Sunn Pedersen, J. Svensson, H. Thomson, Y. Turkin, L. Vano, T. Wauters, G. Wurden, M. Yoshinuma, M. Zanini, and D. Zhang, "Performance of wendelstein 7-X stellarator plasmas during the first divertor operation phase," Phys. Plasmas **26**(8), 082504 (2019).

[15] R. L. Dewar, T. Tatsuno, Z. Yoshida, C. Nührenberg, and B. F. McMillan, "Statistical characterization of the interchange-instability spectrum of a separable ideal-magnetohydrodynamic model system," Phys. Rev. E **70**(6), 066409 (2004).

[16] F. L. Waelbroeck and R. D. Hazeltine, "Stability of low-shear tokamaks," Phys. Fluids **31**(5), 1217–1223 (1988).

[17] R. J. Hastie and T. C. Hender, "Toroidal internal kink stability in tokamaks with ultra flat q profiles," Nucl. Fusion **28**(4), 585 (1988).

[18] L. A. Charlton, B. A. Carreras, and V. E. Lynch, "Linear and nonlinear properties of infernal modes," Phys. Fluids B **2**(7), 1574–1583 (1990).

[19] J. P. Freidberg, Ideal MHD (Cambridge University Press, 2014).

[20] A. M. Wright, N. M. Ferraro, S. R. Hudson, R. L. Dewar, and M. J. Hole, "Predicting nonresonant pressure-driven MHD modes in equilibria with low magnetic shear," Phys. Plasmas **28**(1), 012106 (2021).

[21] J. Manickam, N. Pomphrey, and A. M. M. Todd, "Ideal MHD stability properties of pressure driven modes in low shear tokamaks," Nucl. Fusion **27**(9), 1461–1472 (1987).

[22] S. C. Jardin, N. Ferraro, J. Breslau, and J. Chen, "Multiple timescale calculations of sawteeth and other global macroscopic dynamics of tokamak plasmas," Comput. Sci. Discovery **5**(1), 014002 (2012).

[23] L. E. Zakharov, "The theory of hydromagnetic stability of a tokamak plasma," Nucl. Fusion **18**(3), 335 (1978).

[24] H. Grad, "Toroidal containment of a plasma," Phys. Fluids **10**(1), 137–154 (1967).

[25] I. M. Niven, Diophantine Approximations (Courier Corporation, 2008).

[26] G. H. Hardy and E. M. Wright, An Introduction to the Theory of Numbers (Oxford University Press, 1979).

[27] J. Nührenberg and R. Zille, "Equilibrium and stability of low-shear stellarators," in Proceedings of the Workshop on Theory of Fusion Plasmas (Editrice Compositori, 1987), pp. 3–23.

[28] S. Lang, Introduction to Diophantine Approximations (Springer Science & Business Media, 1995).

[29] A. H. Glasser, "The direct criterion of Newcomb for the ideal MHD stability of an axisymmetric toroidal plasma," Phys. Plasmas **23**(7), 072505 (2016).